Viscoelastic Functionally Graded Materials Subjected to Antiplane Shear Fracture

G. H. Paulino[1]
e-mail: paulino@uiuc.edu
Mem. ASME

Z.-H. Jin
Mem. ASME

Department of Civil and Environmental Engineering,
University of Illinois at Urbana-Champaign,
Newmark Laboratory,
205 North Mathews Avenue,
Urbana, IL 61801

In this paper, a crack in a strip of a viscoelastic functionally graded material is studied under antiplane shear conditions. The shear relaxation function of the material is assumed as $\mu=\mu_0 \exp(\beta y/h) f(t)$, *where h is a length scale and f(t) is a nondimensional function of time t having either the form* $f(t)=\mu_\infty/\mu_0+(1-\mu_\infty/\mu_0)\exp(-t/t_0)$ *for a linear standard solid, or* $f(t)=(t_0/t)^q$ *for a power-law material model. We also consider the shear relaxation function* $\mu=\mu_0 \exp(\beta y/h)[t_0 \exp(\delta y/h)/t]^q$ *in which the relaxation time depends on the Cartesian coordinate y exponentially. Thus this latter model represents a power-law material with position-dependent relaxation time. In the above expressions, the parameters* β, μ_0, μ_∞, t_0; δ, *q are material constants. An elastic crack problem is first solved and the correspondence principle (revisited) is used to obtain stress intensity factors for the viscoelastic functionally graded material. Formulas for stress intensity factors and crack displacement profiles are derived. Results for these quantities are discussed considering various material models and loading conditions.* [DOI: 10.1115/1.1354205]

1 Introduction

Functionally graded materials are the outcome of the need to accommodate materials exposure to nonuniform service requirements. Those materials are characterized by continuously varying properties due to continuous change in *microstructural details* over defined geometrical orientations and distances, such as composition, morphology, and crystal structure. The material gradation may be either continuous or layered comprised, for example, of gradients of ceramics and metals. In applications involving severe thermal gradients (e.g., thermal protection systems), functionally graded material systems take advantage of heat and corrosion resistance typical of ceramics, and mechanical strength and toughness typical of metals. Other relevant applications of functionally graded materials involve polymers ([1]), biomedical systems ([2]), natural composites ([3]), and thermoelectric devices for energy conversion ([4]). Various thermomechanical problems associated to functionally graded materials have been studied, for example, constitutive modeling ([5–7]), higher order theory ([8]), thermal stresses ([9,10]), static and dynamic response of plates ([11]), yield stress gradient effect ([12]), strain gradient theory ([13]), fracture behavior ([14–16]), and statistical model for brittle fracture ([17]).

The antiplane shear crack problem has been extensively studied in the literature as it provides the basis for understanding the opening mode crack problem. Several numerical and analytical/semi-analytical solutions have been presented considering homogeneous materials (e.g., [18,19]), nonhomogeneous materials (e.g., [20,21]), and bonded homogeneous viscoelastic layers ([22]). However, to the best of the authors' knowledge, there is no published analytical/semi-analytical type solution for the problem of an antiplane shear crack in viscoelastic functionally graded materials. This is the subject of this paper, which consists of applying Paulino and Jin's ([23]) revisited correspondence principle for viscoelastic functionally graded materials to fracture mechanics.

One of the primary application areas of functionally graded materials is high-temperature technology. Materials will exhibit creep and stress relaxation behavior at high temperatures. Viscoelasticity offers a basis for the study of phenomenological behavior of creep and stress relaxation. In this paper, viscoelastic fracture (stationary crack) of functionally graded materials is studied under antiplane shear conditions. Specifically, an infinitely long strip containing a crack parallel to the strip boundaries is investigated. The shear relaxation function of the material is assumed to take separable forms in space and time, i.e.,

$$\mu=\mu_0 \exp(\beta y/h) f(t),$$

where h is a length scale and $f(t)$ is a nondimensional function of time t having either the form

$$f(t)=\mu_\infty/\mu_0+(1-\mu_\infty/\mu_0)\exp(-t/t_0): \quad \text{linear standard solid}$$

or

$$f(t)=(t_0/t)^q: \quad \text{power-law material.}$$

We also consider the following variant form of the power-law material model

$$\mu=\mu_0 \exp(\beta y/h)[t_0 \exp(\delta y/h)/t]^q,$$

in which the relaxation time depends on the Cartesian coordinate y exponentially. In the above expressions, the parameters β, μ_0, μ_∞, t_0; δ, q are material constants. An elastic crack problem is first solved and the ''correspondence principle'' is used to obtain the stress intensity factor for the viscoelastic functionally graded material.

This manuscript is organized as follows. The next section presents the basic equations of viscoelasticity theory of functionally graded materials, which are the basis for this study. Then the correspondence principle is revisited and recast in the form recently given by Paulino and Jin [23], followed by a discussion of relaxation functions with separable forms. Next, the antiplane shear problem is formulated together with an integral equation solution approach for a crack in a viscoelastic functionally graded material strip. Formulas for stress intensity factors (as a function

[1]To whom correspondence should be addressed.

Contributed by the Applied Mechanics Division of THE AMERICAN SOCIETY OF MECHANICAL ENGINEERS for publication in the ASME JOURNAL OF APPLIED MECHANICS. Manuscript received by the ASME Applied Mechanics Division, Feb. 24, 2000; final revision, July 13, 2000. Associate Editor: M.-J. Pindera. Discussion on the paper should be addressed to the Editor, Professor Lewis T. Wheeler, Department of Mechanical Engineering, University of Houston, Houston, TX 77204-4792, and will be accepted until four months after final publication of the paper itself in the ASME JOURNAL OF APPLIED MECHANICS.

of geometry, material constants, and loading) are derived considering both Heaviside step function loading and exponentially decaying or increasing loading. Afterwards, the recovery of the displacement field is carried out and applied to obtain the actual crack profile. Several results for the above problem are presented and discussed. Finally, conclusions are inferred and extensions of this work are pointed out. An Appendix, showing the integral equation kernel derivation, supplements the paper.

2 Basic Equations

The basic equations of quasi-static viscoelasticity of functionally graded materials are the equilibrium equation

$$\sigma_{ij,j}=0, \tag{1}$$

the strain-displacement relationship

$$\varepsilon_{ij}=\tfrac{1}{2}(u_{i,j}+u_{j,i}), \tag{2}$$

and the viscoelastic constitutive law

$$s_{ij}=2\int_0^t \mu(\mathbf{x};t-\tau)\frac{de_{ij}}{d\tau}d\tau, \quad \sigma_{kk}=3\int_0^t K(\mathbf{x};t-\tau)\frac{d\varepsilon_{kk}}{d\tau}d\tau, \tag{3}$$

with

$$s_{ij}=\sigma_{ij}-\tfrac{1}{3}\sigma_{kk}\delta_{ij}, \quad e_{ij}=\varepsilon_{ij}-\tfrac{1}{3}\varepsilon_{kk}\delta_{ij}, \tag{4}$$

where σ_{ij} are stresses, ε_{ij} are strains, s_{ij} and e_{ij} are deviatoric components of the stress and strain tensors, respectively, u_i are displacements, δ_{ij} is the Kronecker delta, $\mathbf{x}=(x_1,x_2,x_3)$, $\mu(\mathbf{x},t)$ and $K(\mathbf{x},t)$ are the relaxation functions in shear and dilatation, respectively, t denotes the time, and the Latin indices have the range 1, 2, 3 with repeated indices implying the summation convention. *Note that for functionally graded materials the relaxation functions also depend on spatial positions, whereas in homogeneous viscoelasticity, they are only functions of time, i.e.* $\mu\equiv\mu(t)$ and $K\equiv K(t)$ ([24]).

3 Correspondence Principle Revisited

In general, the correspondence principle of homogeneous viscoelasticity theory does not hold for functionally graded materials. However, for a class of functionally graded materials with relaxation functions of the form

$$\begin{aligned}\mu(\mathbf{x},t)&=\mu_0\tilde{\mu}(\mathbf{x})f(t),\\ K(\mathbf{x},t)&=K_0\tilde{K}(\mathbf{x})g(t),\end{aligned} \tag{5}$$

where μ_0 and K_0 are material constants, and $\tilde{\mu}(\mathbf{x})$, $\tilde{K}(\mathbf{x})$, $f(t)$, and $g(t)$ are nondimensional functions, Paulino and Jin [23] showed that the correspondence principle still holds. In this case, *the Laplace transformed nonhomogeneous viscoelastic solution can be obtained directly from the solution of the corresponding nonhomogeneous elastic problem by replacing* μ_0 *and* K_0 *with* $\mu_0 p\bar{f}(p)$ *and* $K_0 p\bar{g}(p)$, *respectively, where* $\bar{f}(p)$ *and* $\bar{g}(p)$ *are the Laplace transforms of f(t) and g(t), respectively, and p is the transform variable. The final solution is realized upon inverting the transformed solution*.

Among the various models for graded viscoelastic materials are the *standard linear solid* defined by

$$\begin{aligned}\mu(\mathbf{x},t)&=\mu_\infty(\mathbf{x})+[\mu_e(\mathbf{x})-\mu_\infty(\mathbf{x})]\exp\left[-\frac{t}{t_\mu(\mathbf{x})}\right],\\ K(\mathbf{x},t)&=K_\infty(\mathbf{x})+[K_e(\mathbf{x})-K_\infty(\mathbf{x})]\exp\left[-\frac{t}{t_K(\mathbf{x})}\right],\end{aligned} \tag{6}$$

and the *power-law model* given by

$$\mu(\mathbf{x},t)=\mu_e(\mathbf{x})\left[\frac{t_\mu(\mathbf{x})}{t}\right]^q, \quad K(\mathbf{x},t)=K_e(\mathbf{x})\left[\frac{t_K(\mathbf{x})}{t}\right]^q, \quad 0<q<1, \tag{7}$$

where $t_\mu(\mathbf{x})$ and $t_K(\mathbf{x})$ are the relaxation times in shear and bulk muduli, respectively, and q is a material constant. Particular instances of the above models for graded viscoelastic materials may be obtained such that assumption (5) is satisfied. Thus the discussion below indicates the type of revision needed in the general viscoelastic models so that the correspondence principle still holds.

- *Standard linear solid* (6). If the relaxation times t_μ and t_K are constants, if $\mu_e(\mathbf{x})$ and $\mu_\infty(\mathbf{x})$ have the same functional form, and if $K_e(\mathbf{x})$ and $K_\infty(\mathbf{x})$ also have the same functional form, then the model (6) satisfies assumption (5).
- *Power-law model* (7). If the relaxation times t_μ and t_K are independent of spatial position in model (7), then assumption (5) is readily satisfied. Moreover, even if the relaxation times depend on the spatial position in model (7), then the corresponding nonhomogeneous elastic material has the properties

$$\mu=\mu_e(\mathbf{x})[t_\mu(\mathbf{x})]^q, \quad K=K_e(\mathbf{x})[t_K(\mathbf{x})]^q, \tag{8}$$

rather than $\mu=\mu_e(\mathbf{x})$ and $K=K_e(\mathbf{x})$. Thus assumption (5) is satisfied again.

4 Viscoelastic Antiplane Shear Problem

Under antiplane shear conditions, the only nonvanishing field variables are

$$\begin{aligned}u_3(\mathbf{x},t)&=w(x,y;t),\\ \sigma_{31}(\mathbf{x},t)&=\tau_x(x,y;t), \quad \sigma_{32}(\mathbf{x},t)=\tau_y(x,y;t),\\ 2\varepsilon_{31}(\mathbf{x},t)&=\gamma_x(x,y;t), \quad 2\varepsilon_{32}(\mathbf{x},t)=\gamma_y(x,y;t),\end{aligned}$$

with $\mathbf{x}=(x_1,x_2)=(x,y)$. Here new notations for the nonvanishing displacement, stresses, and strains are used for the sake of simplicity. The basic equations of mechanics satisfied by these variables are

$$\frac{\partial\tau_x}{\partial x}+\frac{\partial\tau_y}{\partial y}=0, \tag{9}$$

$$\gamma_x=\frac{\partial w}{\partial x}, \quad \gamma_y=\frac{\partial w}{\partial y}, \tag{10}$$

$$\tau_x=\int_0^t \mu(x,y;t-\tau)\frac{d\gamma_x}{d\tau}d\tau, \quad \tau_y=\int_0^t \mu(x,y;t-\tau)\frac{d\gamma_y}{d\tau}d\tau. \tag{11}$$

In the present study, the following three material models are employed. The first is the *standard linear solid* (see (6)) with constant relaxation time

$$\mu=\mu_0\exp(\beta y/h)\left[\frac{\mu_\infty}{\mu_0}+\left(1-\frac{\mu_\infty}{\mu_0}\right)\exp\left(-\frac{t}{t_0}\right)\right], \tag{12}$$

where β, μ_0, μ_∞, and t_0 are material constants and h is a length scale. The second model is a *power-law material* (see (7)) with *constant relaxation time*

$$\mu=\mu_0\exp(\beta y/h)\left(\frac{t_0}{t}\right)^q. \tag{13}$$

The third model is also a *power-law material* (see (7)), but with *position-dependent relaxation time*

$$\mu=\mu_0\exp(\beta y/h)\left[\frac{t_0\exp(\delta y/h)}{t}\right]^q=\mu_0\exp[(\beta+\delta q)y/h]\left(\frac{t_0}{t}\right)^q, \tag{14}$$

where δ and q are material constants.

5 Relaxation Functions With Separable Forms

The present discussion is based on the main argument that the functional form of the chosen relaxation function(s) is appropriate if the basic constitutents of the functionally graded material have

approximately the same relaxation pattern. Thus this argument indicates the need for an approach integrating mechanics modeling, material properties experiments, and synthesis (see [25] for a review of fabrication processes for functionally graded materials). This point is elaborated upon below.

It can be seen in (12), (13), and (14) that the relaxation moduli are separable functions in space and time. This is necessary for the revisited correspondence principle (see Section 3) to be applied ([23]). This kind of relaxation functions may be appropriate for a functionally graded material with its constituent materials having the same time-dependence of shear modulus. For model (12), this means that the constituents should have the same ratio μ_∞/μ_0 and relaxation time t_0. For model (13), this implies that the constituents should have the same relaxation time t_0 and parameter q. For model (14), however, it is only required that the constituents have the same parameter q. The constituents may have different relaxation times. Potentially, this kind of functionally graded materials may include some polymeric/polymeric materials such as Propylene-homopolymer/Acetal-copolymer. The relaxation behavior of Propylene homopolymer and Acetal copolymer are found to be similar—see Figs. 7.5 and 10.3, respectively, of Ogorkiewicz [26].

Another argument potentially in favor of the selected class of relaxation functions (5) is the technique developed by Lambros et al. [27] for fabricating large scale polymeric functionally graded materials. The technique consists of generating a continuously inhomogeneous property variation by selective ultraviolet irradiation of a polyethylene carbon monoxide copolymer. Due to the fact that the functionally graded material is obtained by controlling ultraviolet irradiation time of the same base polymer, we conjecture that the viscoelastic behavior of such material may be predicted by (5). However, further experimental research needs to be done in order to validate or invalidate the present conjecture.

6 Mode III Crack in a Functionally Graded Material Strip

Consider an infinite nonhomogeneous viscoelastic strip containing a central crack of length $2a$, as shown in Fig. 1. The strip is fixed along the lower boundary ($y=-h$) and is displaced $w(t)=w_0W(t)$ along the upper boundary ($y=h$), where w_0 is a constant and $W(t)$ is a nondimensional function of time t. It is supposed that the crack lies on the x-axis, from $-a$ to a, and is of infinite extent in the z-direction (normal to the x-y plane). The crack surfaces remain traction-free. The boundary conditions of the crack problem, therefore, are

$$w=0, \quad y=-h, \quad |x|<\infty, \tag{15}$$

$$w=w_0W(t), \quad y=h, \quad |x|<\infty, \tag{16}$$

$$\tau_y=0, \quad y=0, \quad |x|\leqslant a, \tag{17}$$

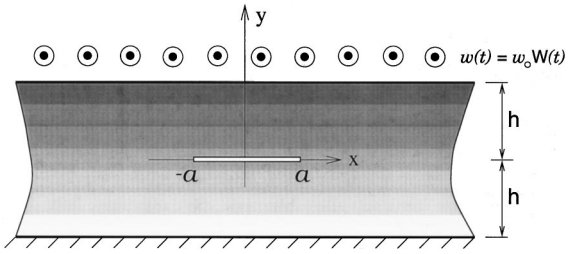

Fig. 1 A viscoelastic functionally graded material strip occupying the region $|x|<\infty$ and $|y|\leqslant h$ with a crack at $|x|\leqslant a$ and $y=0$. The lower boundary of the strip ($y=-h$) is fixed and the upper boundary ($y=h$) is subjected to uniform antiplane displacement $w_0W(t)$. The symbol ⊙ indicates an arrow perpendicular to the strip plane and pointing toward the viewer.

$$\tau_y(x,0^+)=\tau_y(x,0^-), \quad a<|x|<\infty, \tag{18}$$

$$w(x,0^+)=w(x,0^-), \quad a<|x|<\infty. \tag{19}$$

According to the correspondence principle (see Section 3), one can first consider a nonhomogeneous elastic material with the shear modulus

$$\mu=\mu_0\exp(\beta y/h), \tag{20}$$

and the viscoelastic solutions for models (12) and (13) may be obtained by the correspondence principle. For the material model (14) the viscoelastic solution can still be obtained by the correspondence principle provided that the corresponding elastic material has the shear modulus $\mu=\mu_0\exp[(\beta+q\delta)y/h]$ (cf. (5) and (14)).

For the elastic crack problem, the solution consists of a regular solution (for an uncracked strip)

$$w=w(y)=\frac{\exp(\beta)-\exp(-\beta y/h)}{\exp(\beta)-\exp(-\beta)}w_0, \tag{21}$$

$$\tau_x=0, \quad \tau_y=\frac{\beta\mu_0w_0/h}{\exp(\beta)-\exp(-\beta)} \tag{22}$$

and a perturbed solution (by the crack) satisfying the following boundary conditions:

$$w=0, \quad y=\pm h, \quad |x|<\infty, \tag{23}$$

$$\tau_y=-\frac{\beta\mu_0w_0/h}{\exp(\beta)-\exp(-\beta)}, \quad y=0, \quad |x|\leqslant a, \tag{24}$$

$$\tau_y(x,0^+)=\tau_y(x,0^-), \quad a<|x|<\infty, \tag{25}$$

$$w(x,0^+)=w(x,0^-), \quad a<|x|<\infty. \tag{26}$$

The governing differential equation of $w(x,y)$ for the nonhomogeneous elastic material (20) is

$$\nabla^2w+\frac{\beta}{h}\frac{\partial w}{\partial y}=0. \tag{27}$$

By using the Fourier transform method (see, for example, [28]), the boundary value problem described by Eqs. (23) to (27) can be reduced to the following singular integral equation (see Appendix):

$$\int_{-1}^{1}\left[\frac{1}{s-r}+k(r,s,\beta)\right]\varphi(s)ds=-\frac{2\pi\beta w_0/h}{\exp(\beta)-\exp(-\beta)}, \quad |r|\leqslant 1, \tag{28}$$

where the unknown density function $\varphi(r)$ is given by

$$\varphi(x)=\frac{\partial}{\partial x}[w(x,0^+)-w(x,0^-)], \tag{29}$$

the nondimensional coordinates r and s are

$$r=x/a, \quad s=x'/a, \tag{30}$$

respectively, and the Fredholm kernel $k(r,s,\beta)$ is

$$k(x,x',\beta)=a\int_0^\infty P(x,x',\xi,\beta)d\xi \tag{31}$$

with $P(x,x',\beta)$ being given by

$$\begin{aligned}P(x,x',\xi,\beta)=[&\xi(\sqrt{(\beta/h)^2+4\xi^2}-2\xi)-2(\beta^2/h^2+2\xi^2)\\&\times\exp(-\sqrt{\beta^2+4h^2\xi^2})\\&-\xi(2\xi+\sqrt{(\beta/h)^2+4\xi^2})\\&\times\exp(-2\sqrt{\beta^2+4h^2\xi^2})]\end{aligned}$$

$$\times\frac{\sin[(x-x')\xi]}{\xi[1-\exp(-2\sqrt{\beta^2+4h^2\xi^2})]\sqrt{(\beta/h)^2+4\xi^2}}. \quad (32)$$

As expected, in the limit of $h\to\infty$ (free space) and $\beta\to 0$ (homogeneous material case), we obtain that $P(x,x',\xi,\beta)\to 0$. *Moreover, the kernel $k(x,x',\beta)$ is symmetric with respect to β.* Such symmetry will be addressed later in the paper. The function $\varphi(r)$ can be further expressed as

$$\varphi(r)=\psi(r)/\sqrt{1-r^2}, \quad (33)$$

where $\psi(r)$ is continuous for $r\in[-1,1]$. When $\varphi(r)$ is normalized by w_0/h, the elastic Mode III stress intensity factor, K^e_{III}, is obtained as

$$K^e_{\mathrm{III}}=-\mu_0\left(\frac{w_0}{2h}\right)\sqrt{\pi a}\,\psi(1,\beta). \quad (34)$$

Here, the notation $\psi(1,\beta)$ is adopted to emphasize the dependence of $\psi(1)$ on β.

7 Stress Intensity Factors

The stress intensity factors for viscoelastic functionally graded materials satisfying (5) can be obtained using the correspondence principle between the elastic and the Laplace transformed viscoelastic equations. Thus, formulas for stress intensity factors are derived first for general time-dependent loading, and then the results obtained are particularized for exponentially decaying or increasing loading and Heaviside step function loading.

As stated above, for nonhomogeneous viscoelastic materials, the Mode III stress intensity factor, K_{III}, can be obtained by means of the correspondence principle (see Section 3). The upper boundary $y=h$ of the strip is subjected to an antiplane displacement $w_0W(t)$, as illustrated by Fig. 1. In this case, the stress intensity factors for material models (12), (13), and (14) will be

$$K_{\mathrm{III}}=-\mu_0\left(\frac{w_0}{2h}\right)\sqrt{\pi a}\,\psi(1,\beta)\mathcal{L}^{-1}\times\left\{\left[\frac{\mu_\infty}{\mu_0}+\left(1-\frac{\mu_\infty}{\mu_0}\right)\frac{p}{p+1/t_0}\right]\overline{W}(p)\right\}, \quad (35)$$

$$K_{\mathrm{III}}=-\mu_0\left(\frac{w_0}{2h}\right)\sqrt{\pi a}\,\psi(1,\beta)\mathcal{L}^{-1}[t_0^q\Gamma(1-q)p^q\overline{W}(p)], \quad (36)$$

and

$$K_{\mathrm{III}}=-\mu_0\left(\frac{w_0}{2h}\right)\sqrt{\pi a}\,\psi(1,\beta+q\,\delta)\mathcal{L}^{-1}[t_0^q\Gamma(1-q)p^q\overline{W}(p)], \quad (37)$$

respectively, where p is the Laplace transform variable, $\mathcal{L}^{-1}$ represents the inverse Laplace transform, $\overline{W}(p)$ is the Laplace transform of $W(t)$, and $\Gamma(\cdot)$ is the Gamma function.

7.1 Stress Intensity Factors for Exponentially Decaying or Rising Loading. Consider as an example

$$W(t)=\exp(-t/t_L)\to\overline{W}(p)=1/(p+1/t_L) \quad (38)$$

where t_L is a constant measuring the time variation of the load. Note that $t_L>0$ represents an exponentially decaying load, while $t_L<0$ corresponds to an exponentially rising load. This kind of time-dependent loading has been used by Broberg [29]. The stress intensity factors under the loading condition (38) then become

$$K_{\mathrm{III}}=-\mu_0\left(\frac{w_0}{2h}\right)\sqrt{\pi a}\,\psi(1,\beta)F(t), \quad (39)$$

where

$$F(t)=\frac{\mu_\infty}{\mu_0}\exp\left(-\frac{t}{t_L}\right)+\left(1-\frac{\mu_\infty}{\mu_0}\right)\frac{1}{t_0-t_L}\times\left[t_0\exp\left(-\frac{t}{t_L}\right)-t_L\exp\left(-\frac{t}{t_0}\right)\right], \quad (40)$$

for the *standard linear solid* (12), and

$$F(t)=\left(\frac{t_0}{t}\right)^q-\frac{1}{t_L}\int_0^t\left(\frac{t_0}{\tau}\right)^q\exp\left(-\frac{t-\tau}{t_L}\right)d\tau, \quad (41)$$

for the *power-law model* (13).

For the *power-law material with position-dependent relaxation time* (14), the stress intensity factor is

$$K_{\mathrm{III}}=-\mu_0\left(\frac{w_0}{2h}\right)\sqrt{\pi a}\,\psi(1,\beta+q\,\delta)F(t), \quad (42)$$

where $F(t)$ is given in (41).

7.2 Stress Intensity Factors for Heaviside Step Function Loading. For the Heaviside loading conditions,

$$W(t)=H(t)\to\overline{W}(p)=1/p, \quad (43)$$

where $H(t)$ is the Heaviside step function. The stress intensity factors then become (cf. (39))

$$K_{\mathrm{III}}=-\mu_0\left(\frac{w_0}{2h}\right)\sqrt{\pi a}\,\psi(1,\beta)F(t),$$

where $F(t)$ is given by

$$F(t)=\frac{\mu_\infty}{\mu_0}+\left(1-\frac{\mu_\infty}{\mu_0}\right)\exp\left(-\frac{t}{t_0}\right), \quad (44)$$

for the *linear standard solid* (12), and

$$F(t)=\left(\frac{t_0}{t}\right)^q \quad (45)$$

for the *power-law model* (13).

Finally, the stress intensity factor for the *power-law material with position-dependent relaxation time* (14) is given by (cf. (42))

$$K_{\mathrm{III}}=-\mu_0\left(\frac{w_0}{2h}\right)\sqrt{\pi a}\,\psi(1,\beta+q\,\delta)F(t),$$

where $F(t)$ is provided in (45). It is seen that q and δ (parameters describing the position dependence of the relaxation time) affect the stress intensity factor only through the combined parameter $(\beta+q\,\delta)$.

8 Crack Displacement Profile

Accurate representation of the crack profile is relevant in fracture mechanics, especially when the crack-surface displacement is measured experimentally and correlated with results obtained by numerical methods. Thus the crack displacement profile for the problem illustrated in Fig. 1 is recovered in this section. First, general time-dependent loading is considered, and then the formulation is particularized for the Heaviside step function loading and the exponentially decaying or rising loading.

It follows from Eqs. (29) and (33), and the correspondence principle, that the crack-sliding displacement under the time-dependent loading, $w_0 W(t)$, can be expressed by the density function $\varphi(x)$ or $\psi(r)$ (normalized by w_0/h) as follows:

$$[w]=w(x,0^+)-w(x,0^-) =\frac{w_0 W(t)}{h}\int_{-a}^{x}\varphi(x')dx'=w_0 W(t)\left(\frac{a}{h}\right)\int_{-1}^{r}\frac{\psi(s)}{\sqrt{1-s^2}}ds. \tag{46}$$

The displacement at the upper surface of the crack is given by

$$w(x,0^+)=\frac{1}{2}[w]+\frac{1}{2\pi}\left[\frac{w_0 W(t)}{h}\right]\int_{-a}^{a}k_d(x,x')\varphi(x')dx' =\frac{1}{2}[w]+\frac{w_0 W(t)}{2\pi}\left(\frac{a}{h}\right)\int_{-1}^{1}k_d(r,s)\frac{\psi(s)}{\sqrt{1-s^2}}ds, \tag{47}$$

where $k_d(x,x')$ is

$$k_d(x,x')=\int_0^\infty\frac{[-\beta+2\beta\exp(-\sqrt{\beta^2+4h^2\xi^2})-\beta\exp(-2\sqrt{\beta^2+4h^2\xi^2})]}{\sqrt{(\beta/h)^2+4\xi^2}[1-\exp(-2\sqrt{\beta^2+4h^2\xi^2})]}\times\frac{\sin[(x-x')\xi]}{\xi}d\xi. \tag{48}$$

Note that the displacements are not symmetric with respect to β (see Fig. 1), however, the stress intensity factors are (cf. (28) and (32)). The displacement at the lower crack surface is then given by

$$w(x,0^-)=w(x,0^+)-[w]. \tag{49}$$

In expressions (46) and (47), $W(t)$ is given in (38) for the exponentially decaying or rising load. For the Heaviside step function load, $W(t)$ is given by (43).

9 Numerical Aspects

To obtain the numerical solution of integral Eq. (28), $\psi(r)$ is expanded into a series of Chebyshev polynomials of the first kind. By noting the relationship (33) between $\varphi(r)$ and $\psi(r)$, $\varphi(r)$ is expressed as follows (Erdogan et al. [28]):

$$\varphi(r)=\frac{1}{\sqrt{1-r^2}}\sum_{n=1}^{\infty}a_n T_n(r),\quad |r|\leqslant 1, \tag{50}$$

where $T_n(r)$ are Chebyshev polynomials of the first kind and a_n are unknown constants. By substituting the above equation into integral Eq. (28), we have

$$\sum_{n=1}^{\infty}\{\pi U_{n-1}(r)+H_n(r)\}a_n=-\frac{\pi\beta w_0/h}{\exp(\beta)-\exp(-\beta)},\quad |r|\leqslant 1, \tag{51}$$

where $U_{n-1}(r)$ are Chebyshev polynomials of the second kind and $H_n(r)$ are given by

$$H_n(r)=\int_{-1}^{1}ak(r,s,\beta)\frac{T_n(s)}{\sqrt{1-s^2}}ds. \tag{52}$$

To solve the functional Eq. (51), the series on the left side is first truncated at the Nth term. A collocation technique is then used and the collocation points, r_i, are chosen as the roots of the Chebyshev polynomials of the first kind

$$r_i=\cos\frac{(2i-1)\pi}{2N},\quad i=1,2,\ldots,N. \tag{53}$$

The functional Eq. (51) is then reduced to a linear algebraic equation system

$$\sum_{n=1}^{N}\{\pi U_{n-1}(r_i)+H_n(r_i)\}a_n=-\frac{\pi\beta w_0/h}{\exp(\beta)-\exp(-\beta)},\quad i=1,2,\ldots,N. \tag{54}$$

After $a_n(n=1,2,\ldots,N)$ are determined, the nondimensional stress intensity factor, $-\psi(1,\beta)$, is computed as follows:

$$-\psi(1,\beta)=-\sum_{n=1}^{N}a_n. \tag{55}$$

In the following numerical calculations, it is found that 20 collocation points lead to a convergent stress intensity factor result.

It is known from (39) that the stress intensity factor is a multiplification of three parts. The first term is a dimensional base, $\mu_0(w_0/2h)\sqrt{\pi a}$, *the second term is a geometrical and material nonhomogeneity correction factor,* $-\psi(1,\beta)$, *which can be obtained from the numerical solution of singular integral Eq. (28), and the third term is the time evolution of stress intensity factor, F(t), which is obtained analytically from the inverse Laplace transform.*

Note that, according to Fig. 1, the crack is located at midheight of the material strip and the origin of the coordinate system (x,y) is located at the center of the crack. Such choice of reference system introduces certain symmetries in the solution, which are discussed in the examples below.

10 Results

Numerical results for stress intensity factors are first obtained for a homogeneous elastic strip (see Fig. 1). According to Table 1, the stress intensity factors are found in good agreement with those reported in the literature, e.g., the handbook by Tada et al. [30]. Furthermore, for a homogeneous viscoelastic strip, it is evident that the stress intensity factor is given by (39) with $\beta=0$ and $F(t)$ is given by (40) and (41) for the exponentially decaying or rising loading, and by (44) and (45) for the Heaviside step function loading. Note that the function $F(t)$ is not related to the nonhomogeneous material parameter β.

Figure 2 shows normalized stress intensity factor (see (39)), $-\psi(1,\beta)$, versus the nonhomogeneous parameter β considering various strip thicknesses h/a for the linear standard solid (12) and the power-law model with constant relaxation time (13). Note that although the relaxation times are different for both models

Table 1 Mode III stress intensity factors (SIF) for a homogeneous strip

h/a	SIF (this study)	SIF ([30])
0.5	0.5360	0.5631
1.0	0.7598	0.7641
1.5	0.8626	0.8634
2.0	0.9136	0.9138
5.0	0.9840	0.9840
10.0	0.9959	0.9959

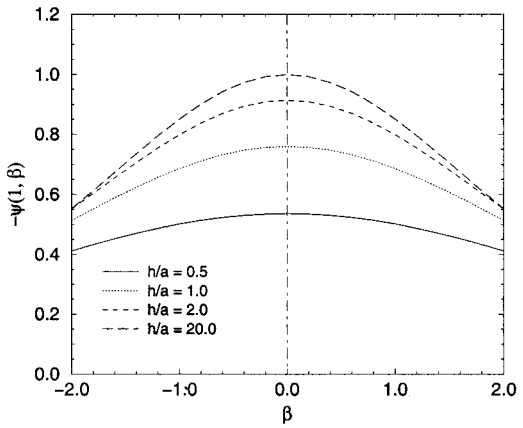

Fig. 2 Normalized Mode III stress intensity factor versus nonhomogeneous material parameter β for various strip thicknesses considering the linear standard solid and the power-law material with constant relaxation time

(cf. Eqs. (40) and (41), or Eqs. (44) and (45)), they do have the same solution $-\psi(1,\beta)$ (see Section 5). The stress intensity factor decreases with increasing $|\beta|$ for all thickness cases (h/a) considered. The stress intensity factor is lower than that of the corresponding homogeneous material ($\beta=0$). It is noted that the stress intensity factor is an even function of β. However, this symmetry is valid only for the crack located in the center of the strip.

Figure 3 shows normalized stress intensity factor (see (42)), $-\psi(1,\beta+q\delta)$, versus the nonhomogeneous parameter β for various strip thicknesses h/a and three δ values for the power-law model with position-dependent relaxation time (14). The effect of spatial position dependence of the relaxation time on the stress intensity factor is reflected through the parameter δ. The parameter q is taken as 0.4 in all calculations. Thus the curves for $\delta=\pm1$ may be obtained from the curve $\delta=0$ by shifting this curve by $\beta=\mp0.4$. It is clear from Fig. 3 that with respect to the corresponding model with constant relaxation time (i.e., $\delta=0$), a positive δ lowers the stress intensity factor when $\beta>0$ and increases the stress intensity factor for β less than $-0.5q\delta$. A negative δ lowers the stress intensity factor when $\beta<0$ and increases the stress intensity factor for β larger than $0.5q\delta$.

Figure 4 illustrates the time evolution of normalized stress intensity factors, $F(t)$, considering both Heaviside step function loading and exponentially decaying or rising loading for the standard linear solid (see (40) and (44)) and the power-law material (see (41) and (45)). The ratio μ_∞/μ_0 is taken as 0.5 in all subsequent calculations for the standard linear solid. It is evident that under the fixed displacement condition, stress intensity factor decreases monotonically with increasing time for Heaviside step function loading and exponentially decaying loading (Figs. 4(*a*) and 4(*b*)). For exponentially rising loading, however, the stress intensity factors will increase with time for longer times (Figs. 4(*c*) and 4(*d*)). By observing the plots in Figs. 4(*a*) and 4(*b*), one notices that, for exponentially decaying loading, the stress intensity factor can become negative as the ratio t_L/t_0 decreases, which occurs, for example, for $t_L/t_0=1.0$. This happens because of stress relaxation for long-time behavior. *Note that a negative stress intensity factor does not imply crack closure because it is*

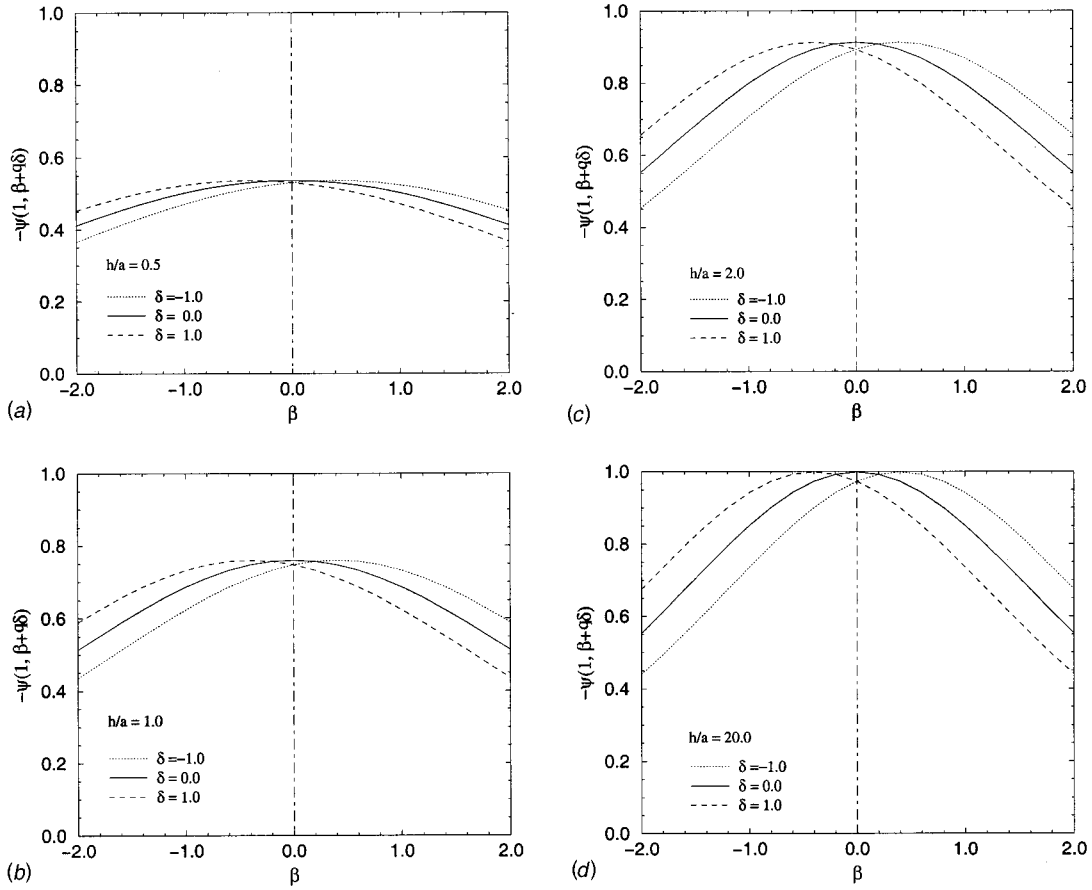

Fig. 3 Normalized Mode III stress intensity factors versus nonhomogeneous parameter β for three δ values and $q=0.4$, (*a*) $h/a=0.5$; (*b*) $h/a=1.0$; (*c*) $h/a=2.0$; (*d*) $h/a=20.0$

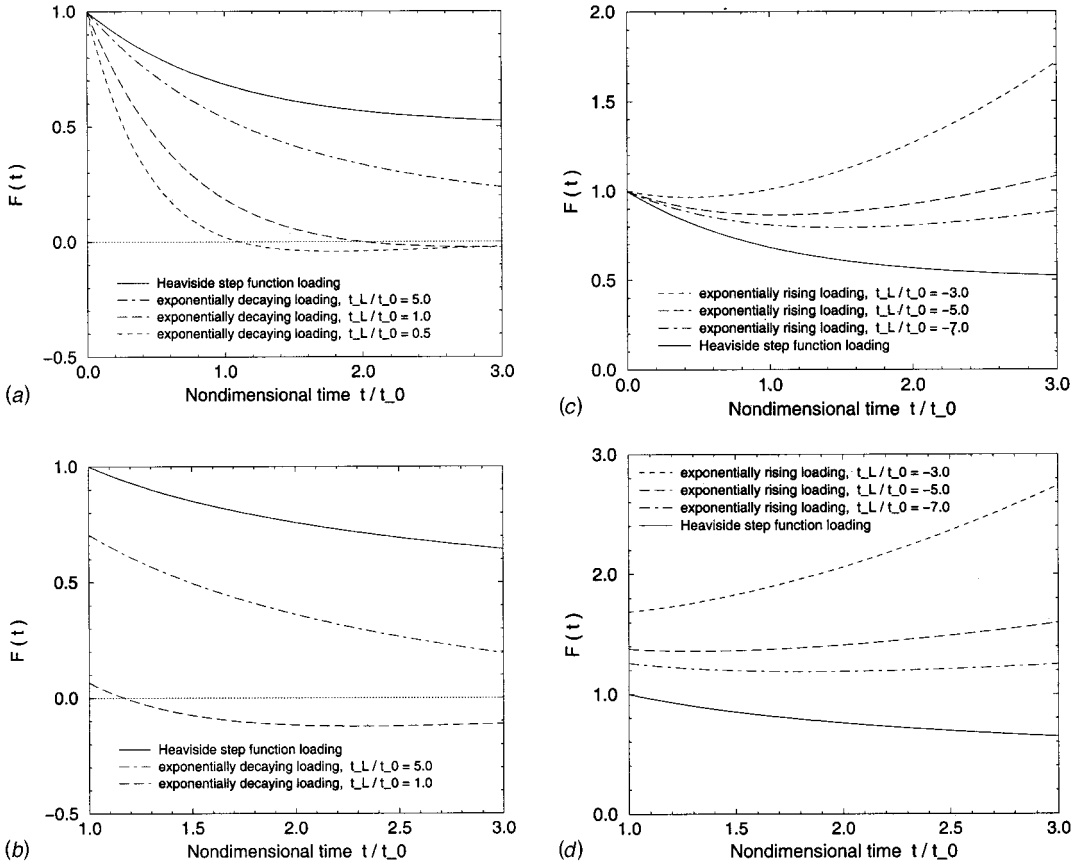

Fig. 4 Time variation of normalized Mode III stress intensity factor (*a*) standard linear solid (decaying loading); (*b*) power-law material (decaying loading); (*c*) standard linear solid (rising loading); (*d*) power-law material (rising load)

associated to a Mode III crack, and not a Mode I (or mixed mode) crack. Thus, in the present study, a negative stress intensity factor is allowed without violating the crack face traction free condition. The crack faces do not close, they just slide in the opposite direction.

Figure 5 illustrates the normalized stress intensity factors (normalized by $\mu_0(w_0/2h)\sqrt{\pi a}$) versus time for Heaviside step function loading considering the following viscoelastic material models: standard linear solid (see (39) and (44)), power law material (see (39) and (45)), and power-law material with position-dependent relaxation time (see (42) and (45)). A finite thickness strip with $h/a=2.0$ (Fig. 1) is considered. Note that, for all the models, the stress intensity factors decrease monotonically with increasing time. The first two models are investigated for the nonhomogeneous parameter $\beta=0$, 1, 2 with $\beta=0$ corresponding to the homogeneous material case. Due to the symmetry of stress intensity factor about β, the stress intensity factor for $\beta=-1$, -2 are identical to those for $\beta=1$, 2, respectively. Moreover, the stress intensity factor decreases with increasing $|\beta|$. The last model is investigated for $\beta=2$ and $\delta=-1,0,1$ with $\delta=0$ corresponding to position-independent relaxation time. For this special case, the stress intensity factor decreases with increasing δ. This is because $\beta+q\delta$ is positive for the β and δ values considered.

Figure 6 illustrates the normalized stress intensity factors (normalized by $\mu_0(w_0/2h)\sqrt{\pi a}$) versus time for exponentially decaying loading considering the following models: standard linear solid (see (39) and (40)), power-law material (see (39) and (41)), and power-law material with position-dependent relaxation time (see (42) and (41)). The same qualitative observations for Fig. 5 also hold for Fig. 6.

Figure 7 presents the normalized stress intensity factors (normalized by $\mu_0(w_0/2h)\sqrt{\pi a}$) versus time for exponentially rising loading for the standard linear solid (see (39) and (40)). Comparing this figure with Figs. 5(*a*) and 6(*a*) (Heaviside step function loading and exponentially decaying loading), one observes that the time variation of stress intensity factors show a convex shape in Fig. 7 while it shows a monotonically decreasing trend in Figs. 5(*a*) and 6(*a*).

Figure 8 shows crack profiles for the Heaviside step function loading considering the standard linear solid and the power law material with position-dependent relaxation time (see (46), (47), and (49)). A finite thickness strip geometry with $h/a=2$ (Fig. 1) is considered. The former model (Fig. 8(*a*)) is investigated for the nonhomogeneity parameter $\beta=0$, 1, 2 with $\beta=0$ corresponding to the homogeneous material case. The latter model (Fig. 8(*b*)) is investigated for $\beta=2$ and $\delta=-1$, 0, 1 with $\delta=0$ corresponding to position-independent relaxation time.

Figure 9 shows crack profiles for the exponentially decaying loading considering the standard linear solid and the power-law material with position-dependent relaxation time (see (46), (47), and (49)). As before, a finite thickness strip geometry with $h/a=2$ (Fig. 1) is considered. The former model (Fig. 9(*a*)) is investigated for the nonhomogeneity parameter $\beta=2$ and $t/t_0=1$, 2, 3. The latter model (Fig. 9(*b*)) is investigated for $\beta=2$, $\delta=1$, and $t/t_0=1$, 2, 3. A comparison of all the plots in Figs. 8 and 9 permits to evaluate the corresponding crack profiles for various material models and various parameters. This information is potentially valuable when correlated with fracture experiments, e.g., crack-sliding displacement measurements.

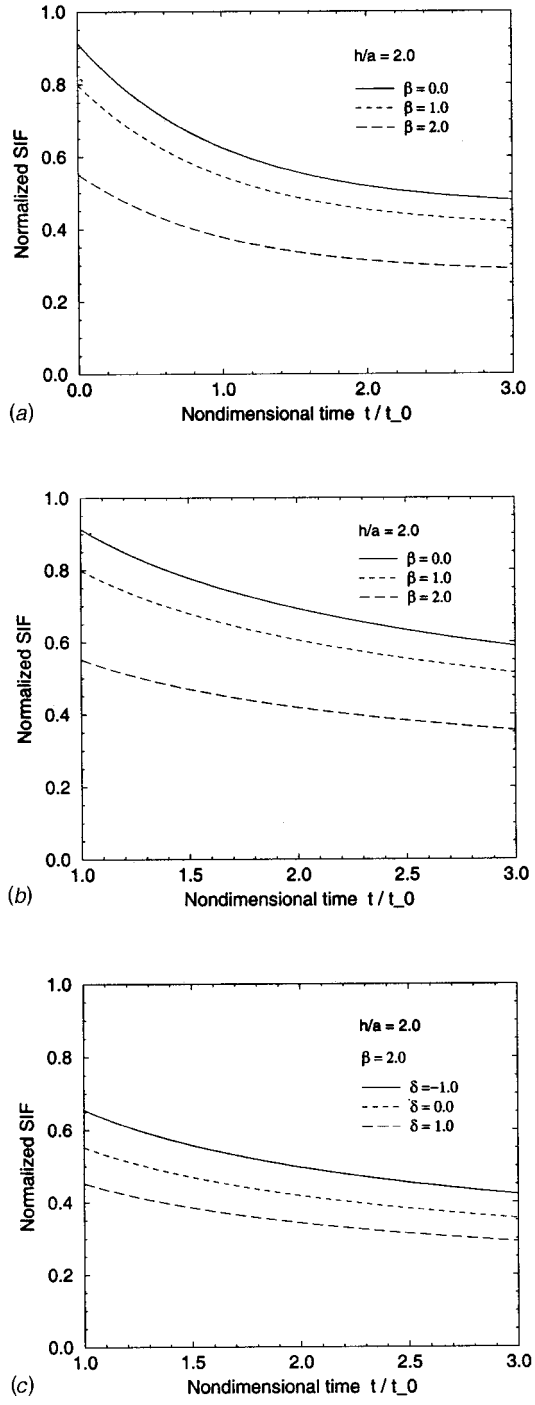

Fig. 5 Normalized Mode III stress intensity factor versus time: Heaviside step function loading, (*a*) standard linear solid; (*b*) power-law material; (*c*) power-law material with position-dependent relaxation time

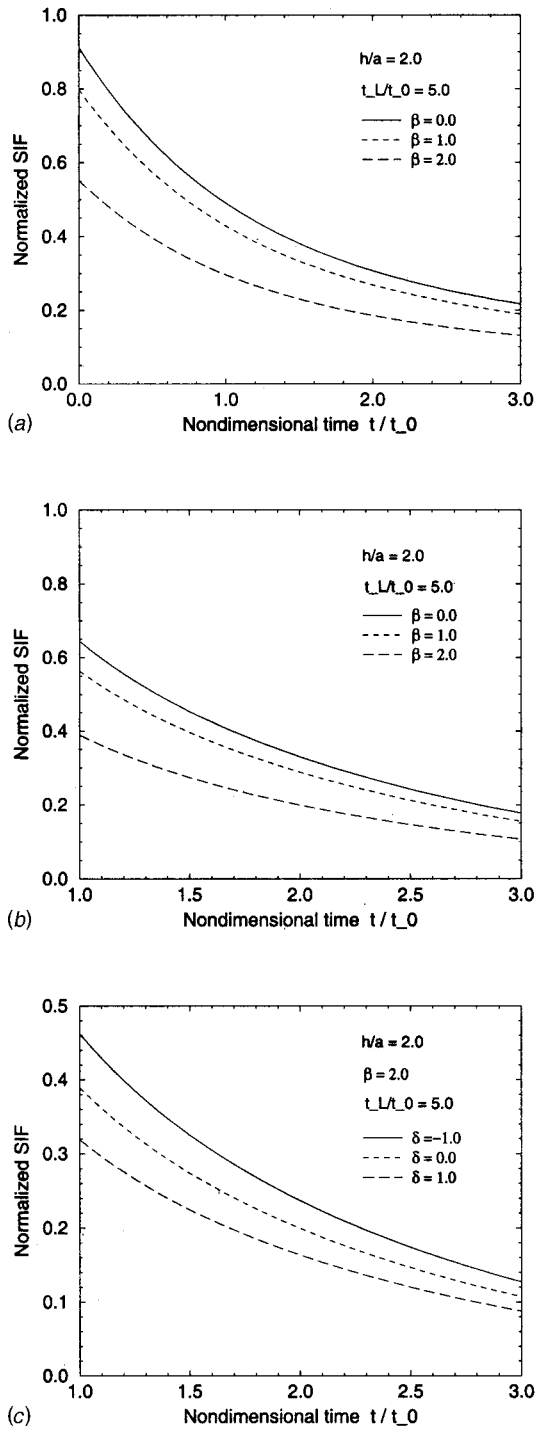

Fig. 6 Normalized mode III stress intensity factor versus time: exponentially decaying loading, (*a*) standard linear solid; (*b*) power-law material; (*c*) power-law material with position-dependent relaxation time

11 Concluding Remarks and Extensions

This paper illustrates an application of Paulino and Jin's [23] revisited correspondence principle to fracture mechanics of viscoelastic functionally graded materials. An effective integral equation method for antiplane shear cracking in viscoelastic functionally graded materials is presented. The elastic functionally graded material crack problem is solved and the correspondence principle between the elastic and the Laplace transformed viscoelastic equations is used to obtain stress intensity factors for viscoelastic functionally graded materials. Formulas for stress intensity factors and crack displacement profiles are provided. Several numerical results for these quantities are presented considering various viscoelastic material models (e.g., standard linear solid, power-law model with both position-independent and position-dependent relaxation time) and loading conditions. It is important to remark that the solution of the fracture mechanics problem with prescribed displacement (see Fig. 1) is different from the solution with prescribed traction (cf. Erdogan [15,20]).

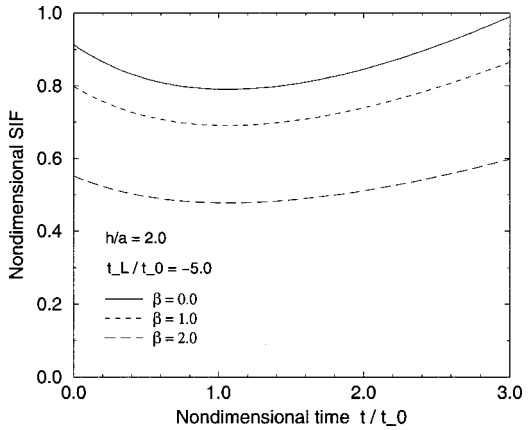

Fig. 7 Normalized Mode III stress intensity factor versus time: exponentially rising loading (standard linear solid)

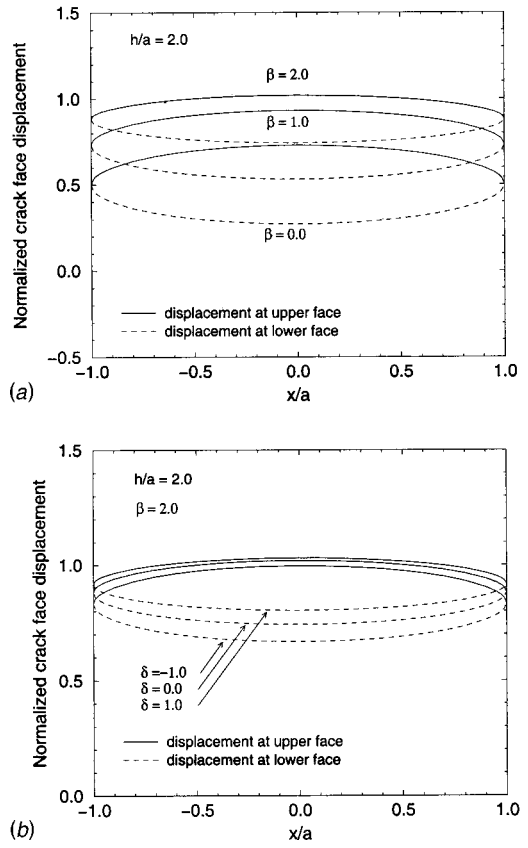

Fig. 8 Crack face displacements: Heaviside step function loading, (*a*) standard linear solid; (*b*) power-law material with position-dependent relaxation time

This work offers promising avenues for further extension. For instance, it may be used to calibrate numerical methods (e.g., finite element method and boundary element method) for viscoelastic functionally graded materials. Moreover, the discussion on relaxation functions of separable forms in space and time (Section 5) indicates the need for micromechanics models for viscoelastic behavior. Other relevant topics associated with this work also deserve further investigation. Such topics include: (a) investigation of antiplane shear cracking in bonded viscoelastic layers where one of the layers is a functionally graded material; (b) extension of the antiplane shear crack model to Mode I cracks. These topics are presently being pursued by the authors.

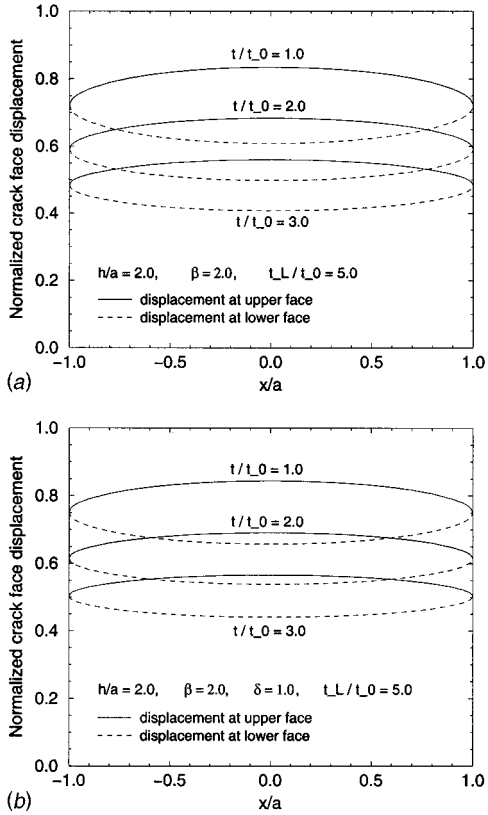

Fig. 9 Crack face displacements: exponentially decaying loading, (*a*) standard linear solid; (*b*) power-law material with position-dependent relaxation time

Acknowledgments

We would like to acknowledge Professor Pindera and four anonymous reviewers for their valuable comments regarding our work. We also acknowledge the support from the National Science Foundation (NSF) under grant No. CMS-9996378 (Mechanics & Materials Program).

Appendix

In the following, a relatively detailed derivation of integral Eq. (28) is given, which refers to the Mode III fracture mechanics problem illustrated by Fig. 1. By using Fourier transform, the solution of the basic Eq. (27) can be expressed as follows:

$$w=\frac{1}{\sqrt{2\pi}}\int_{-\infty}^{\infty}\left\{A_1\exp\left[\frac{-\beta+m}{2}\frac{y}{h}\right]+A_2\exp\left[\frac{-\beta-m}{2}\frac{y}{h}\right]\right\}\times\exp(-ix\xi)d\xi,\quad y>0,$$

$$w=\frac{1}{\sqrt{2\pi}}\int_{-\infty}^{\infty}\left\{B_1\exp\left[\frac{-\beta+m}{2}\frac{y}{h}\right]+B_2\exp\left[\frac{-\beta-m}{2}\frac{y}{h}\right]\right\}\times\exp(-ix\xi)d\xi,\quad y<0, \tag{56}$$

where A_1, A_2, B_1, and B_2 are unknowns, and m is

$$m\equiv m(\xi)=\sqrt{\beta^2+4h^2\xi^2}. \tag{57}$$

The stress τ_y is obtained from (56) by Hooke's law,

$$\tau_y=\mu_0\exp(\beta y/h)\frac{\partial w}{\partial y}$$
$$=\frac{\mu_0\exp(\beta y/h)}{\sqrt{2\pi}}\int_{-\infty}^{\infty}\left\{\frac{-\beta+m}{2h}A_1\exp\left[\frac{-\beta+m}{2}\frac{y}{h}\right]+\frac{-\beta-m}{2h}A_2\exp\left[\frac{-\beta-m}{2}\frac{y}{h}\right]\right\}\exp(-ix\xi)d\xi,\quad y>0,$$
$$\tau_y=\mu_0\exp(\beta y/h)\frac{\partial w}{\partial y}$$
$$=\frac{\mu_0\exp(\beta y/h)}{\sqrt{2\pi}}\int_{-\infty}^{\infty}\left\{\frac{-\beta+m}{2h}B_1\exp\left[\frac{-\beta+m}{2}\frac{y}{h}\right]+\frac{-\beta-m}{2h}B_2\exp\left[\frac{-\beta-m}{2}\frac{y}{h}\right]\right\}\exp(-ix\xi)d\xi,\quad y<0. \tag{58}$$

By using the boundary conditions (23) to (26), the unknowns A_2, B_1, and B_2 can be expressed by A_1 which is given by

$$A_1=\frac{1}{i\xi}\left\{1-\exp(m)-[1-\exp(-m)]\times\frac{-\beta+m+(\beta+m)\exp(m)}{-\beta+m+(\beta+m)\exp(-m)}\right\}\times\frac{1}{\sqrt{2\pi}}\int_{-a}^{a}\varphi(x')\exp(ix'\xi)dx', \tag{59}$$

where $\varphi(x)$ is the density function defined by

$$\varphi(x)=\frac{\partial}{\partial x}[w(x,0^+)-w(x,0^-)]. \tag{60}$$

Further, the stress τ_y at $y=0$ is expressed by $\varphi(x)$ as

$$\tau_{y|y=0}=\frac{\mu_0}{2\pi}\int_{-a}^{a}\left[\frac{1}{x'-x}+k(x,x',\beta)\right]\varphi(x')dx' \tag{61}$$

where $k(x,x',\beta)$ is given in (31). By substituting the above expression into the boundary condition (24), the integral Eq. (28) is deduced.

References

[1] Orihara, K., 1999, ''Self-Assembly of Functionally Graded Plastics by a Particular Phase Separation of Polymer Blend and Its Applications,'' *Fifth U.S. National Congress on Computational Mechanics, Book of Abstracts*, pp. 399–400.

[2] Pompe, W., Lampenscherf, S., Rössler, S., Scharnweber, D., Weis, K., Worch, H., and Hofinger, J., 1999, ''Functionally Graded Bioceramics,'' Mater. Sci. Forum, **308–311**, pp. 325–330.

[3] Nogata, F., and Takahashi, H., 1995, ''Intelligent Functionally Graded Material: Bamboo,'' Composites Eng., **5**, pp. 743–751.

[4] Hirano, T., Teraki, J., and Nishio, Y., 1999, ''Computational Design for Functionally Graded Thermoelectric Materials,'' Mater. Sci. Forum, **308–311**, pp. 641–646.

[5] Reiter, T., Dvorak, G. J., and Tvergaard, V., 1997, ''Micromechanical Models for Graded Composite Materials,'' J. Mech. Phys. Solids, **45**, pp. 1281–1302.

[6] Reiter, T., and Dvorak, G. J., 1998, ''Micromechanical Models for Graded Composite Materials: II. Thermomechanical Loading,'' J. Mech. Phys. Solids, **46**, pp. 1655–1673.

[7] Gasik, M. M., 1998, ''Micromechanical Modelling of Functionally Graded Materials,'' Comput. Mater. Sci., **13**, pp. 42–55.

[8] Aboudi, J., Pindera, M. J., and Arnold, S. M., 1999, ''Higher-Oder Theory for Functionally Graded Materials,'' Composites, Part B, **30B**, pp. 777–832.

[9] Kawasaki, A., and Watanabe, R., 1987, ''Finite Element Analysis of Thermal Stress of the Metals/Ceramics Multi-Layer Composites with Controlled Compositional Gradients,'' J. Jpn. Inst. Met., **51**, pp. 525–529.

[10] Noda, N., 1999, ''Thermal Stresses in Functionally Graded Materials,'' J. Therm. Stresses, **22**, pp. 477–512.

[11] Praveen, G. N., and Reddy, J. N., 1998, ''Nonlinear Transient Thermoelastic Analysis of Functionally Graded Ceramic-Metal Plates,'' Int. J. Solids Struct., **35**, pp. 4457–4476.

[12] Kolednik, O., 2000, ''The Yield Stress Gradient Effect in Inhomogeneous Materials,'' Int. J. Solids Struct., **37**, pp. 781–808.

[13] Paulino, G. H., Fannjiang, A. C., and Chan, Y. S., 1999, ''Gradient Elasticity Theory for a Mode III Crack in a Functionally Graded Material,'' Mater. Sci. Forum, **308–311**, pp. 971–976.

[14] Cai, H., and Bao, G., 1998, ''Crack Bridging in Functionally Graded Coatings,'' Int. J. Solids Struct., **35**, pp. 701–717.

[15] Erdogan, F., 1995, ''Fracture Mechanics of Functionally Graded Materials,'' Composites Eng., **5**, pp. 753–770.

[16] Jin, Z.-H., and Batra, R. C., 1996, ''Some Basic Fracture Mechanics Concepts in Functionally Graded Materials,'' J. Mech. Phys. Solids, **44**, pp. 1221–1235.

[17] Becker, Jr., T. L., Cannon, R. M., and Ritchie, R. O., 1999, ''A Statistical RKR Fracture Model for the Brittle Fracture of Functionally Graded Materials,'' Mater. Sci. Forum, **308–311**, pp. 957–962.

[18] Rice, J. R., 1968, ''Mathematical Analysis in the Mechanics of Fracture,'' *Fracture—An Advanced Treatise*, Vol. II, H. Liebowitz, ed., Pergamon Press, Oxford, pp. 191–311.

[19] Paulino, G. H., Saif, M. T. A., and Mukherjee, S., 1993, ''A Finite Elastic Body With a Curved Crack Loaded in Anti-Plane Shear,'' Int. J. Solids Struct., **30**, pp. 1015–1037.

[20] Erdogan, F., 1985, ''The Crack Problem for Bonded Nonhomogeneous Materials Under Antiplane Shear Loading,'' ASME J. Appl. Mech., **52**, pp. 823–828.

[21] Ang, W. T., Clements, D. L., and Cooke, T., 1999, ''A Hypersingular Boundary Integral Equation for Antiplane Crack Problems for a Class of Inhomogeneous Anisotropic Elastic Materials,'' Eng. Anal. Boundary Elem., **23**, pp. 567–572.

[22] Atkinson, C., and Chen, C. Y., 1996, ''The Influence of Layer Thickness on the Stress Intensity Factor of a Crack Lying in an Elastic (Viscoelastic) Layer Embedded in a Different Elastic (Viscoelastic) Medium (Mode III Analysis),'' Int. J. Eng. Sci., **34**, pp. 639–658.

[23] Paulino, G. H., and Jin, Z.-H., 2001, ''Correspondence Principle in Viscoelastic Functionally Graded Materials,'' ASME J. Appl. Mech., **68**, pp. 129–132.

[24] Christensen, R. M., 1971, *Theory of Viscoelasticity*, Academic Press, New York.

[25] Hirai, T., 1996, ''Functionally Gradient Materials,'' *Materials Science and Technology, 17B: Processing of Ceramics, Part 2* R. J. Brook, ed., VCH Verlagsgesellschaft mbH, Weinheim, Germany, pp. 292–341.

[26] Ogorkiewicz, R. M., 1970, *Engineering Properties of Thermoplastics*, John Wiley and Sons, London.

[27] Lambros, J., Santare, M. H., Li, H., and Sapna, III, G. H., 1999, ''A Novel Technique for the Fabrication of Laboratory Scale Model Functionally Graded Materials,'' Exp. Mech., **39**, pp. 184–190.

[28] Erdogan, F., Gupta, G. D., and Cook, T. S., 1973, ''Numerical Solution of Singular Integral Equations,'' *Mechanics of Fracture*, Vol. 1, G. C. Sih, ed., Noordhoff, Leyden, pp. 368–425.

[29] Broberg, K. B., 1999, *Cracks and Fracture*, Academic Press, London.

[30] Tada, H., Paris, P., and Irwin, G., 1973, *The Stress Analysis of Cracks Handbook*, Del Research Corporation, Helletown, PA.